

ORIGINAL ARTICLE

# hMENA<sup>11a</sup> contributes to HER3-mediated resistance to PI3K inhibitors in HER2-overexpressing breast cancer cells

P Trono<sup>1</sup>, F Di Modugno<sup>1</sup>, R Circo<sup>2</sup>, S Spada<sup>1,3</sup>, A Di Benedetto<sup>4</sup>, R Melchionna<sup>1</sup>, B Palermo<sup>1,3</sup>, S Matteoni<sup>5</sup>, S Soddu<sup>5</sup>, M Mottolese<sup>4</sup>, R De Maria<sup>6</sup> and P Nisticò<sup>1</sup>

Human Mena (hMENA), an actin regulatory protein of the ENA/VASP family, cooperates with ErbB receptor family signaling in breast cancer. It is overexpressed in high-risk preneoplastic lesions and in primary breast tumors where it correlates with HER2 overexpression and an activated status of AKT and MAPK. The concomitant overexpression of hMENA and HER2 in breast cancer patients is indicative of a worse prognosis. hMENA is expressed along with alternatively expressed isoforms, hMENA<sup>11a</sup> and hMENA $\Delta$ v6 with opposite functions. A novel role for the epithelial-associated hMENA<sup>11a</sup> isoform in sustaining HER3 activation and pro-survival pathways in HER2-overexpressing breast cancer cells has been identified by reverse phase protein array and validated *in vivo* in a series of breast cancer tissues. As HER3 activation is crucial in mechanisms of cell resistance to PI3K inhibitors, we explored whether hMENA<sup>11a</sup> is involved in these resistance mechanisms. The specific hMENA<sup>11a</sup> depletion switched off the HER3-related pathway activated by PI3K inhibitors and impaired the nuclear accumulation of HER3 transcription factor FOXO3a induced by PI3K inhibitors, whereas PI3K inhibitors activated hMENA<sup>11a</sup> phosphorylation and affected its localization. At the functional level, we found that hMENA<sup>11a</sup> sustains cell proliferation and survival in response to PI3K inhibitor treatment, whereas hMENA<sup>11a</sup> silencing increases molecules involved in cancer cell apoptosis. As shown in three-dimensional cultures, hMENA<sup>11a</sup> contributes to resistance to PI3K inhibition because its depletion drastically reduced cell viability upon treatment with PI3K inhibitor BEZ235. Altogether, these results indicate that hMENA<sup>11a</sup> in HER2-overexpressing breast cancer cells sustains HER3/AKT axis activation and contributes to HER3-mediated resistance mechanisms to PI3K inhibitors. Thus, hMENA<sup>11a</sup> expression can be proposed as a marker of HER3 activation and resistance to PI3K inhibition therapies, to select patients who may benefit from these combined targeted treatments. hMENA<sup>11a</sup> activity could represent a new target for antiproliferative therapies in breast cancer.

*Oncogene* advance online publication, 11 May 2015; doi:10.1038/onc.2015.143

## INTRODUCTION

Members of the ErbB family have a crucial role in breast cancer (BC) formation and progression. Identification of the mechanisms involved in their complex signaling network has led to the development of ErbB-specific inhibitors<sup>1</sup> that have improved the outcome of patients with HER2-positive tumors; however, a number of patients develop resistance to these drugs. One of the proposed resistance mechanisms involves reactivation of PI3K signaling via alternative receptor tyrosine kinase amplified pathways and/or mutations in the PI3K pathway.<sup>2</sup> Several antagonists of the PI3K pathway have been entered in phase I and II clinical trials.<sup>3</sup> However, their clinical efficacy is strongly impaired by compensatory feedback mechanisms that lead to upregulation and activation of multiple receptor tyrosine kinase and, finally, to drug resistance.<sup>4,5</sup>

HER3 is a critical signaling node in the ErbB family and its activation contributes to cellular adaptation to PI3K inhibitors in HER2-overexpressing tumors.<sup>5–7</sup> In HER2-driven cancers, HER3 is an important heterodimer partner that binds the PI3K regulatory subunits and activates the PI3K/AKT survival pathway,<sup>8–10</sup> suggesting that the co-inhibition of HER3 and PI3K pathways may exert a greater antitumor efficacy.<sup>7</sup>

Actin cytoskeleton and its organization are strongly deregulated in cancer and affect many signaling pathways related to relevant cell functions, such as apoptosis, adhesion and migration.<sup>11</sup> Human Mena (hMENA) belongs to the ENA/VASP protein family with key roles in cellular processes governed by the actin dynamics.<sup>12,13</sup> hMENA, overexpressed in 70% of BC with HER2+, ER/PgR– and high Ki67 phenotype and correlated with an activated status of MAPK and AKT kinases, has been reported as an early marker of breast tumorigenesis.<sup>14,15</sup> The concomitant overexpression of HER2 and hMENA identifies a subgroup of BC patients with a worse prognosis.<sup>15</sup> The *MENA* gene encodes the 570-aa hMENA protein and different splicing-derived isoforms have been reported in human<sup>16,17</sup> and mouse.<sup>12,18,19</sup> Two isoforms, epithelial specific hMENA<sup>11a</sup> and mesenchymal specific hMENA $\Delta$ v6, with opposing regulatory functions in tumor cell invasion are differentially expressed in primary BC.<sup>20</sup> hMENA and hMENA<sup>11a</sup> are upregulated by epidermal growth factor (EGF) and Neuregulin (NRG-1) growth factor that specifically phosphorylate hMENA<sup>11a</sup>, whereas Trastuzumab treatment downregulates hMENA expression and inhibits hMENA<sup>11a</sup> phosphorylation.<sup>15,16</sup> Depletion of all hMENA isoforms reduces HER3 phosphorylation, inhibits EGF- and NRG-1-mediated phosphorylation of EGF-Receptor (EGFR) and HER2, and impairs growth factor-mediated

<sup>1</sup>Laboratory of Immunology, Experimental Oncology, Regina Elena National Cancer Institute, Rome, Italy; <sup>2</sup>Department of Hematology, Oncology and Molecular Medicine, Istituto Superiore di Sanità, Rome, Italy; <sup>3</sup>Department of Molecular Medicine, Sapienza, University of Rome, Rome, Italy; <sup>4</sup>Department of Pathology, Regina Elena National Cancer Institute, Rome, Italy; <sup>5</sup>Experimental Oncology, Regina Elena National Cancer Institute, Rome, Italy and <sup>6</sup>Scientific Direction, Regina Elena National Cancer Institute, Rome, Italy. Correspondence: Dr P Nisticò, Laboratory of Immunology, Regina Elena National Cancer Institute, Via Elio Chianesi 53, Rome, 00144 Italy. E-mail: nistico@ifo.it

cell proliferation.<sup>15</sup> Given the role of hMENA<sup>11a</sup> isoform in tumor cell proliferation and its cross talk with ErbB receptors,<sup>15</sup> we set up a phospho-proteomic analysis to investigate the role of hMENA<sup>11a</sup> in different oncogenic signaling pathways related to proliferation and survival. Here, we show that the hMENA<sup>11a</sup> overexpression correlates with HER3 and P-HER3 in HER2-overexpressing BC tissues. In HER2+ BC cells, our results indicate that hMENA<sup>11a</sup> is an anti-apoptotic regulator involved in the HER3-mediated mechanisms of resistance to PI3K inhibition.

**RESULTS**

RPPA analysis reveals that hMENA<sup>11a</sup> silencing inhibits HER3/AKT activation in MDA-MB-361 cells

To examine the role of hMENA<sup>11a</sup> overexpression on oncogenic signaling pathways related to cell proliferation and survival, we set up a reverse phase protein array (RPPA) analysis of 85 proteins and phospho-proteins (Supplementary Figure 1). We compared the phospho-proteomic profiles of the luminal BC cell line MDA-MB-361, which overexpresses HER2 and hMENA/hMENA<sup>11a</sup>, before and after hMENA<sup>11a</sup>-specific silencing (MDA-MB-361 si-CNTR vs

MDA-MB-361 si-hMENA<sup>11a</sup>). The hMENA<sup>11a</sup> silencing specifically downregulates the hMENA<sup>11a</sup> protein level, but does not modify the hMENA protein level (Supplementary Figure 2). The heatmap in Figure 1a shows the hierarchical clustering of 59 significant endpoints; MDA-MB-361 control cells displayed a sustained activation of several oncogenic pathways, for example, HER2 and EGFR, and a moderate activation of HER3. hMENA<sup>11a</sup> silencing significantly downregulated the phosphorylation of EGFR (Y1068 and Y1148), HER2 (Y1248) and HER3 (Y1289); among other receptor tyrosine kinases, it reduced the activation levels of cKit, Met and ALK, indicating that hMENA<sup>11a</sup> plays a critical role in sustaining the activation of different oncogenic signals. A number of survival proteins, such as survivin, were downregulated by hMENA<sup>11a</sup> silencing, while proteins such as H2AX and the cleaved forms of PARP and CASP9, all features of the apoptotic process, were upregulated. Overall, these RPPA data evidence a crucial role of hMENA<sup>11a</sup> in sustaining signaling pathways related to cell proliferation and survival.

NRG-1 promotes hMENA<sup>11a</sup> overexpression and phosphorylation,<sup>15</sup> thus we performed RPPA analysis on MDA-MB-361 cells (si-CNTR and si-hMENA<sup>11a</sup>) after NRG-1 treatment. A strong increase of

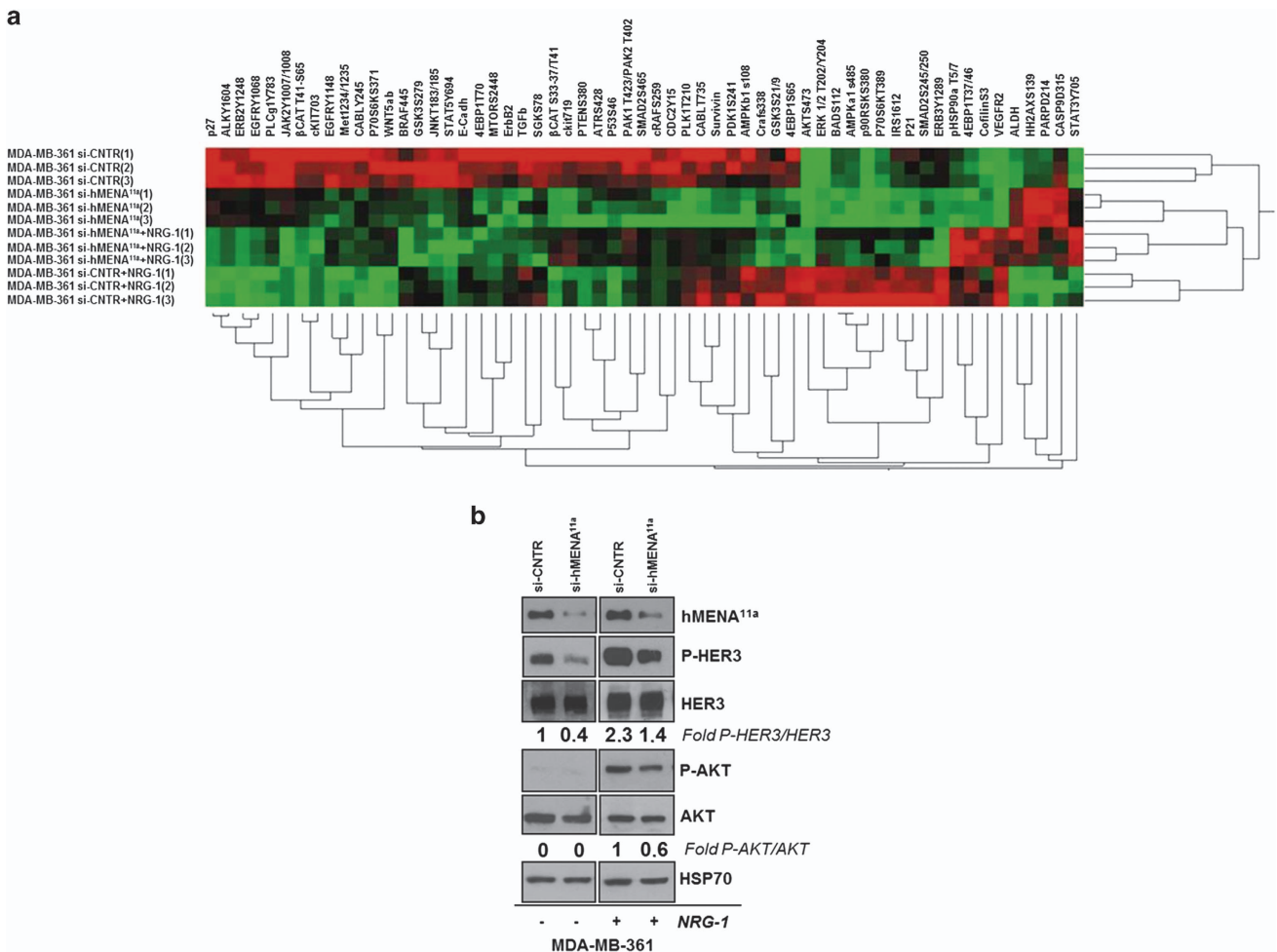


**Figure 1.** RPPA analysis reveals that hMENA<sup>11a</sup> sustains HER3/AKT axis in MDA-MB-361 cells. **(a)** Two-way unsupervised hierarchical clustering analysis (average method) for 59 proteins with significant differences ( $P < 0.05$ , Dunnett's test) in MDA-MB-361 cells transfected with nontargeting si-RNA (si-CNTR) and hMENA<sup>11a</sup>-specific si-RNAs (si-hMENA<sup>11a</sup>), serum starved overnight and untreated or treated with 10 nM NRG-1 for 24 h. Red color represents the higher relative levels of activity/expression, black the intermediate levels and green the lower relative levels of activity/expression. Experiment was performed in biological triplicates indicated as 1, 2, 3 in the heatmap. **(b)** Validation of RPPA results by WB analysis for P-HER3 and P-AKT. Densitometric quantitation of protein bands was determined by NIH ImageJ software. P-HER3 signals were normalized in comparison with total HER3 and fold increase or decrease is indicated with respect to si-CNTR-untreated cells. P-AKT signals were normalized in comparison with total AKT and fold decrease is indicated with respect to si-CNTR NRG-1-treated sample. HSP70 was used as the loading control.

HER3 activation, paralleled by a slight reduction of HER2 and EGFR phosphorylation, occurred in MDA-MB-361 cells treated with NRG-1 (Figure 1a), suggesting that NRG-1 preferentially elicits HER3 and downstream targets AKT (S473) and p70S6K (T389) phosphorylation. Of note, NRG-1 treatment also increased insulin receptor substrate 1 (IRS1) phosphorylation, as previously reported for ER+ BC cell lines.<sup>21</sup> Differently, as evidenced in the heatmap (Figure 1a), hMENA<sup>11a</sup> silencing impairs NRG-1-mediated activation of the HER3/AKT axis. These results were validated by western blot (WB) (Figure 1b).

When we assessed whether HER3 could reciprocally affect hMENA<sup>11a</sup> expression, we evidenced that HER3 silencing does not affect hMENA<sup>11a</sup> expression either in MDA-MB-361 or in MCF7 cells transfected with HER2 (MCF7-HER2) (Supplementary Figure 2).

Overall, phospho-proteomic analysis and its WB validation revealed that hMENA<sup>11a</sup> sustains HER3 activation and its downstream, pro-survival AKT pathway, suggesting a role for this hMENA isoform in survival and proliferation signals.

hMENA<sup>11a</sup> expression correlates with HER3 expression and phosphorylation in HER2-overexpressing BC patients

To investigate whether the strong correlation between hMENA<sup>11a</sup> and HER3 activation evidenced by RPPA analysis occurs also *in vivo*, hMENA<sup>11a</sup> isoform expression was evaluated by immunohistochemistry in parallel with HER3 and Y1289 P-HER3 antibodies in a series of 49 HER2-positive invasive ductal breast carcinomas consecutively selected from the surgical pathology files of the Regina Elena National Cancer Institute (Rome, Italy) with the approval of the Ethical Committee and written informed consent obtained from all patients. Clinicopathologic information of patients is listed in Supplementary Table 4.

Ninety-five percent of cases showing a 2+, 3+ P-HER3 score (for representative scores, see Supplementary Figure 3) were concomitantly positive for hMENA<sup>11a</sup> ( $P \leq 0.0001$ ), evidencing a strong correlation between hMENA<sup>11a</sup> and HER3 activation (Table 1). Although to a lesser extent, HER3 expression also correlates with hMENA<sup>11a</sup> expression ( $P = 0.008$ ) (data not shown). A phosphorylated status of HER3 was evidenced in 61% of the 31 HER3-positive cases (Supplementary Table 5). Representative cases stained with hMENA<sup>11a</sup>, HER3 and P-HER3 antibodies are reported in Figure 2.

Of note, cases which evidence a strong HER3 phosphorylation (score 2+, 3+) show an intense membranous staining of hMENA<sup>11a</sup>, whereas, when P-HER3 is negative or low scored (score 0, 1+), staining of hMENA<sup>11a</sup> is diffuse and cytoplasmic, leading us to hypothesize that the hMENA<sup>11a</sup> relocalization is suggestive of a still to be elucidated function, related to HER3 activation. These *in vivo* results indicate that hMENA<sup>11a</sup> overexpression is associated with HER3 activation in BC tissues and may represent a useful marker of HER3 activity.

hMENA<sup>11a</sup> silencing impairs HER3 activation and FOXO3a-mediated HER3 upregulation induced by PI3K inhibitors

Given the critical role of HER3 in drug resistance and in treatment failure of PI3K inhibitors,<sup>7</sup> we investigated whether hMENA<sup>11a</sup> is involved in the mechanisms of HER3-mediated resistance to PI3K inhibitors in HER2-overexpressing BC cells. To test this hypothesis, MCF7-HER2 cells harboring constitutive activation of PI3K (E545K PIK3CA) were specifically silenced for hMENA<sup>11a</sup> and treated with the dual PI3K/mTOR inhibitor BEZ235.<sup>22</sup> WB analyses showed that HER3 and AKT were constitutively active in MCF7-HER2 control cells (si-CNTR) (Figure 3a). hMENA<sup>11a</sup> silencing reduced P-HER3 and P-AKT levels without affecting their expression. As expected, treatment with BEZ235 (24 h) completely inhibited P-AKT and P-S6. Consistent with previous reports,<sup>4,7</sup> the drug upregulated HER3 expression and activation. However, when the cells were silenced for hMENA<sup>11a</sup>, the effect of BEZ235 treatment on HER3 was impaired (Figure 3a). Similar results were obtained upon BEZ235 treatment of MDA-MB-361 cells (Supplementary Figure 4).

**Table 1.** hMENA<sup>11a</sup> strongly correlates with HER3 phosphorylation status (P-HER3) in HER2-positive breast carcinomas

P-HER3	hMENA <sup>11a</sup>		Total cases	P value
	Positive 2+/3+	Negative 0/1+		
Positive 2+/3+	18 (95%)	1 (5%)	19	< 0.0001
Negative 0/1+	11 (37%)	19 (63%)	30	
Total cases	29 (59%)	20 (41%)	49	

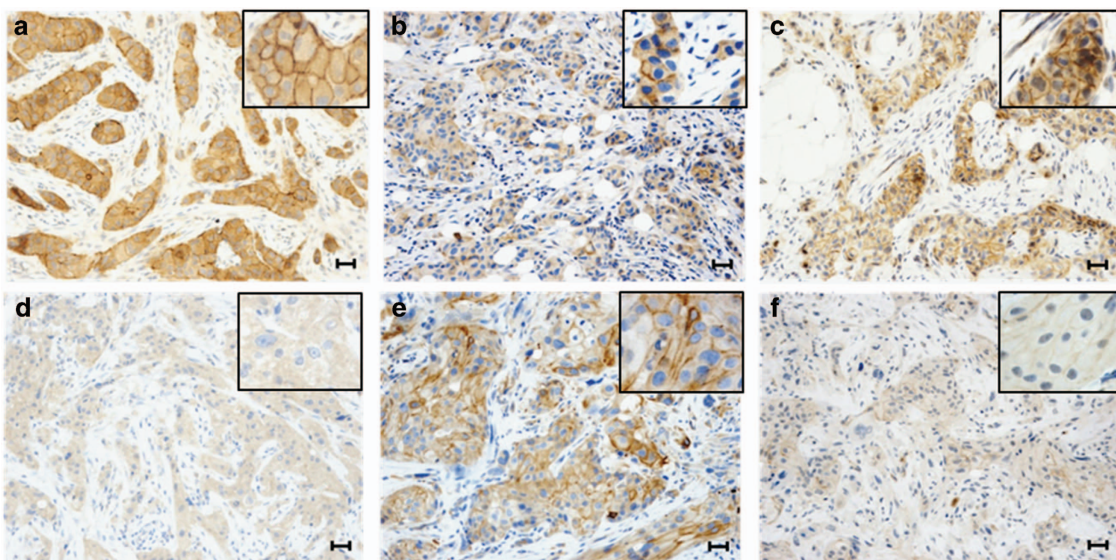


**Figure 2.** hMENA<sup>11a</sup> expression correlates with P-HER3 in HER2-positive BC. hMENA<sup>11a</sup>, HER3 and P-HER3 staining of two representative cases by immunohistochemistry is reported: panels a–c display a strong immunoreactivity against (a) hMENA<sup>11a</sup>, (b) HER3 and (c) P-HER3; panels d–f show (d) a low hMENA<sup>11a</sup> expression, (e) a strong HER3 staining and (f) a low P-HER3 staining. Scale bar 30 μm. Inset magnification × 40.

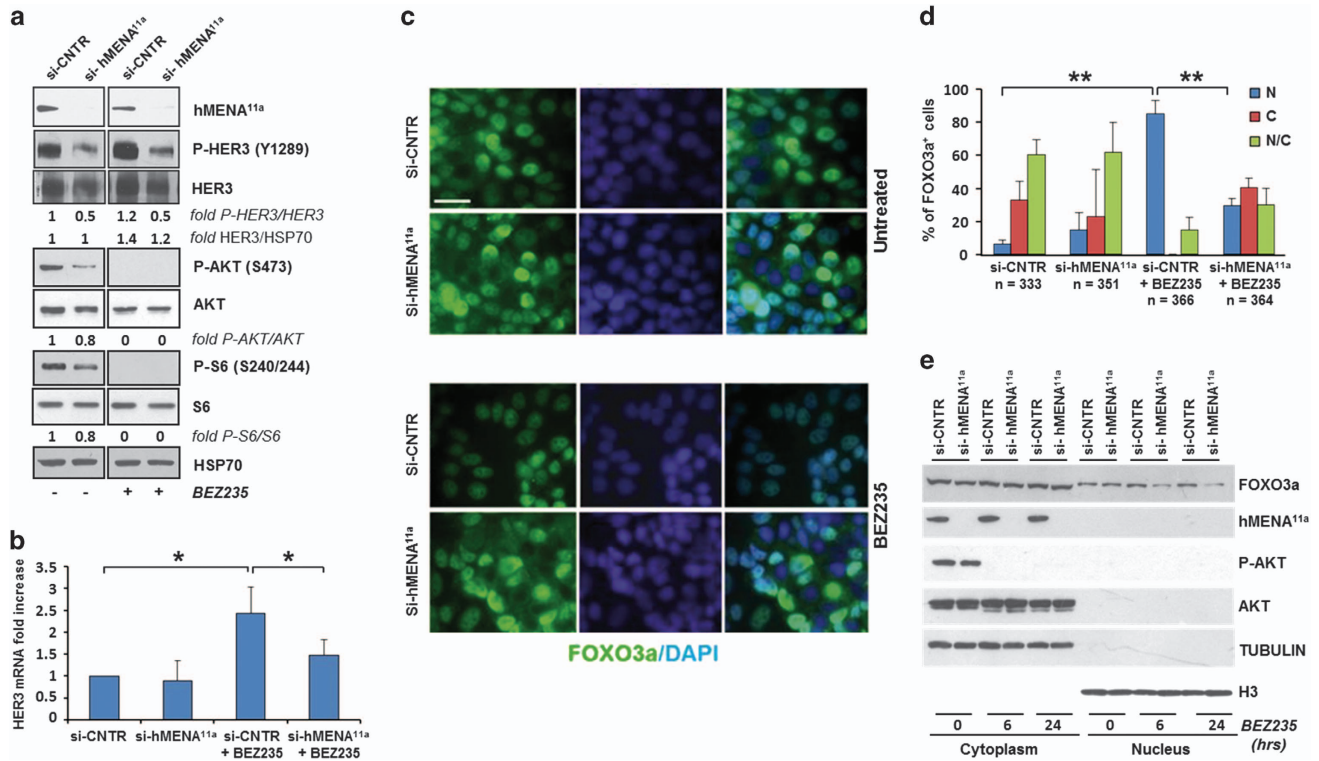


**Figure 3.** hMENA<sup>11a</sup> silencing impairs HER3 activation and FOXO3a-mediated HER3 upregulation induced by PI3K inhibitors. **(a)** Lysates from MCF7-HER2 cells transfected with nontargeting si-RNA (si-CNTR) or hMENA<sup>11a</sup>-specific si-RNAs (si-hMENA<sup>11a</sup>) and treated with 0.5  $\mu$ M BEZ235 in 10% fetal calf serum containing medium for 24 h, were immunoblotted against the indicated antibodies. HSP70 was used as the loading control. Densitometric quantitation of protein bands was determined by NIH ImageJ software. P-HER3, P-AKT and P-S6 signals were normalized in comparison with total HER3, AKT and S6 signals, respectively; HER3 signals were normalized in comparison with HSP70. Fold increase or decrease were calculated with respect to si-CNTR-untreated cells. **(b)** Real-time qPCR with HER3-specific primers of RNA from MCF7-HER2 cells transfected with si-CNTR and hMENA<sup>11a</sup>-specific siRNAs untreated and treated with 0.5  $\mu$ M BEZ235 for 24 h. All experiments were repeated three times, each time in triplicate. Each bar represents the mean  $\pm$  s.d. of three independent experiments. \* $P \leq 0.05$ . **(c)** Subcellular distribution of FOXO3a determined by immunofluorescence analysis of MCF7-HER2 cells transfected with si-CNTR and hMENA<sup>11a</sup>-specific si-RNAs and treated with 0.5  $\mu$ M BEZ235 for 24 h. Cells were stained with FOXO3a antibody (green) and nuclei were visualized by 4',6-diamidino-2-phenylindole (blue). Magnification  $\times 63$ . Scale bar 30  $\mu$ m. **(d)** Quantification of the FOXO3a subcellular distribution patterns, nuclear (N), cytoplasmic (C) or nuclear and cytoplasmic (N/C), is shown as the mean  $\pm$  s.d. of three experiments. \*\*\* $P \leq 0.01$ . **(e)** WB analysis of cytoplasmic and nuclear fractions of MCF7-HER2 si-CNTR and si-hMENA<sup>11a</sup> cells, untreated or treated with 0.5  $\mu$ M BEZ235 for 6 and 24 h and subjected to nuclear and cytoplasmic fractionation. Lysates were immunoblotted against the indicated antibodies. Histone H3 and tubulin were used as loading controls of nuclear and cytoplasmic fractions, respectively.

By qRT-PCR, we quantified the levels of *HER3* mRNA in MCF7-HER2 cells upon PI3K inhibition by either BEZ235 (Figure 3b) or LY294002 (ref 23) (Supplementary Figure 4b). The *HER3* mRNA upregulation mediated by PI3K inhibition was impaired by hMENA<sup>11a</sup> silencing, whereas no effect was evident in untreated cells (Figure 3b), in agreement with data at protein level.

PI3K inhibitors increase *HER3* transcription through deregulation of the transcription factor FOXO3a.<sup>5,24</sup> FOXO3a nuclear translocation is impaired by AKT-mediated phosphorylation, whereas downregulation of P-AKT due to PI3K inhibition results in FOXO3a nuclear accumulation and increase of *HER3* transcription.<sup>5,24</sup>

Thus, we asked whether hMENA<sup>11a</sup> overexpression may affect FOXO3a subcellular localization by analyzing MCF7-HER2 control cells (si-CNTR) and hMENA<sup>11a</sup>-silenced cells (si-hMENA<sup>11a</sup>) untreated or BEZ235-treated. In the majority of the untreated cells, FOXO3a was simultaneously found in both nucleus and cytoplasm, and hMENA<sup>11a</sup> silencing did not modify FOXO3a localization (Figure 3c). As expected, BEZ235 treatment resulted in FOXO3a nuclear accumulation in 85% of si-CNTR cells followed by *HER3* mRNA upregulation (Figures 3d and b). Differently, hMENA<sup>11a</sup> silencing impaired BEZ235-mediated FOXO3a nuclear accumulation (Figure 3c). Only 29% of cells showed a FOXO3a

nuclear localization (Figure 3d). Similar results were obtained in MDA-MB-361 cells by using three different PI3K inhibitors (Supplementary Figure 4c).

These immunofluorescence results were confirmed by biochemical experiments on fractionated cell lysates evidencing that nuclear accumulation of FOXO3a upon BEZ235 treatment was impaired in silenced hMENA<sup>11a</sup> cells, at 24 h and even at short incubation (6 h) (Figure 3e). Taken together, these data suggest that hMENA<sup>11a</sup> sustains the PI3K inhibition-mediated *HER3* upregulation, at least in part, by allowing FOXO3a nuclear accumulation.

#### PI3K inhibitor treatment affects hMENA<sup>11a</sup> phosphorylation and localization

To investigate the functional role of hMENA<sup>11a</sup> in the compensatory pathways involved in the resistance to PI3K inhibitors, we analyzed whether BEZ235 treatment affects hMENA<sup>11a</sup> expression levels and we found that the treatment does not modify hMENA<sup>11a</sup> expression levels (Figure 4a).

However, immunofluorescence analysis evidenced a different subcellular localization of hMENA<sup>11a</sup> in the untreated (CNTR) vs PI3K inhibitor-treated cells. A diffuse cytoplasmic pattern of

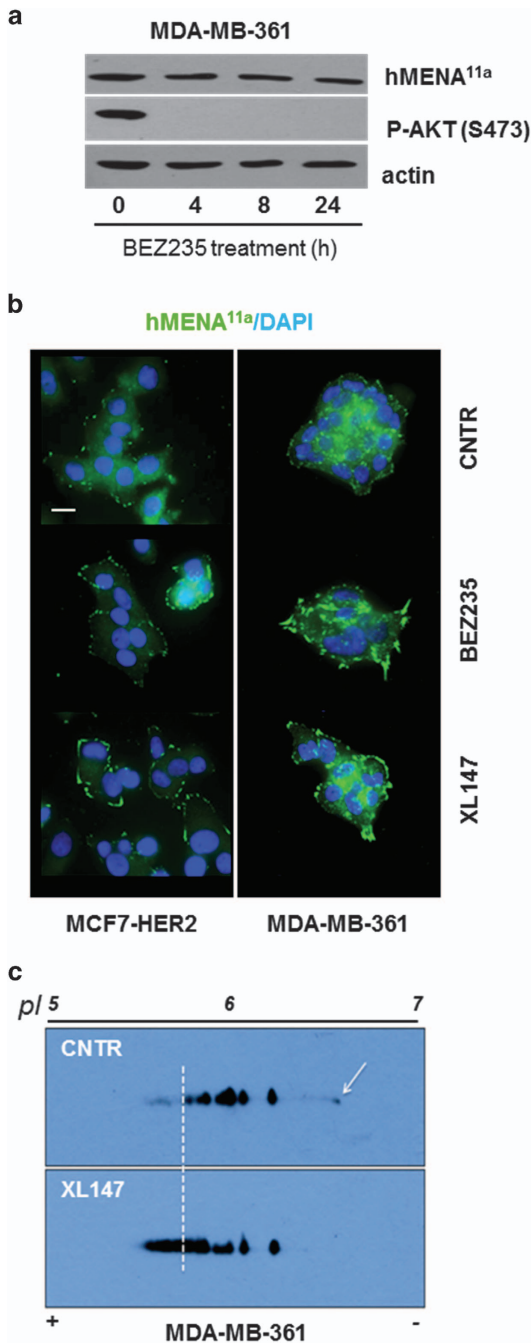


**Figure 4.** hMENA<sup>11a</sup> is phosphorylated and relocated by PI3K inhibitor treatment. **(a)** Lysates from MDA-MB-361 cells treated with 0.5  $\mu$ M BEZ235 for 4, 8 and 24 h, were immunoblotted against hMENA<sup>11a</sup> and P-AKT antibodies. Actin antibody was used as the loading control. **(b)** Immunofluorescence analysis of MCF7-HER2 and MDA-MB-361 cells untreated or treated with 0.5  $\mu$ M BEZ235 (24 h) and 20  $\mu$ M XL147 (16 h). Cells were stained with hMENA<sup>11a</sup>-specific antibody (green), nuclei with 4'6-diamidino-2-phenylindole (blue). Magnification  $\times$ 63. Scale bar 20  $\mu$ m. **(c)** 2D-electrophoresis on a pH 4–7 nonlinear range and 10% acrylamide SDS–PAGE of protein extracts from MDA-MB-361 cells untreated (CNTR) or treated with 20  $\mu$ M XL147 (XL147). Proteins were electrophoretically transferred to nitrocellulose and then incubated with hMENA<sup>11a</sup> antibody; the shift toward acidic pH of the hMENA<sup>11a</sup>-specific spots is indicated by a dashed line. The arrow indicates hMENA<sup>11a</sup>-positive spots in MDA-MB-361 CNTR that disappear after XL147 treatment.

hMENA<sup>11a</sup> was revealed in the CNTR cells, whereas PI3K inhibitors determined hMENA<sup>11a</sup> translocation to the membrane, where it appears to be organized in structures reminiscent of focal adhesions (Figure 4b).

hMENA<sup>11a</sup> is phosphorylated by EGF and NRG-1 mitogenic signals, whereas Trastuzumab significantly downregulates hMENA<sup>11a</sup> phosphorylation, suggesting a cross talk between hMENA<sup>11a</sup> and EGFR family signaling.<sup>15</sup> Thus, we speculated that different hMENA<sup>11a</sup> localization might be related to its phosphorylation status. A two-dimensional electrophoresis conducted on MDA-MB-361 untreated (CNTR) or treated with the PI3K inhibitor (XL147)<sup>25</sup> showed that the inhibitor determined a shift of hMENA<sup>11a</sup> spots toward an acidic pH, a pattern reminiscent of that previously reported for hMENA<sup>11a</sup> phosphorylation induced by EGF or NRG-1 stimulation (Figure 4c).

hMENA<sup>11a</sup> sustains cancer cell proliferation, survival and resistance to HER3-mediated PI3K inhibition

Results that hMENA<sup>11a</sup> overexpression might affect AKT-related pro-survival signaling pathways prompted us to verify the role of hMENA<sup>11a</sup> overexpression at the functional level. We stably transfected hMENA<sup>11a</sup> in DAL (thereafter called DAL11a), a breast cancer cell line with undetectable expression of any of the hMENA isoforms.<sup>26</sup> In DAL11a, the P-HER3 levels were increased, confirming a link between hMENA<sup>11a</sup> and HER3 activation in BC cells (Figure 5a). Of note, the hypothesis that only the epithelial hMENA<sup>11a</sup> isoform is linked to HER3 signaling was confirmed by transfecting DAL cells with the mesenchymal-related hMENA $\Delta$ v6 isoform<sup>20</sup> that did not affect HER3 activation levels (Figure 5b). To evaluate whether hMENA<sup>11a</sup> overexpression affects cell proliferation and survival in response to BEZ235 treatment, we evaluated dose–response curves in DAL and DAL11a cells. hMENA<sup>11a</sup> overexpression determined a shift in BEZ235 IC<sub>50</sub> from 67 nM in DAL compared with 111 nM in DAL11a after 72 h of treatment, indicating that hMENA<sup>11a</sup> may be crucial in the resistance of BC cells to BEZ235 treatment (Figure 5c).

We further evaluated cell cycle distribution by flow cytometry. hMENA<sup>11a</sup> silencing impacted on cell proliferation of both MDA-MB-361 and MCF7-HER2, decreasing the percentage of cells in the S phase and increasing those in the G1 phase of the cell cycle (Figure 6a). In agreement with previous observations,<sup>27</sup> BEZ235 treatment resulted in an accumulation of cells in the G1 phase compared with the untreated controls (Figure 6a). Of relevance, the combination of hMENA<sup>11a</sup> silencing and BEZ235 treatment further decreased the percentage of cells in the S phase (Figure 6a) and induced the accumulation of a sub-G1 peak (Figure 6b, upper panel), suggestive of cell death. These data were confirmed by <sup>3</sup>H-thymidine incorporation assay (Supplementary Figure 5).

To evaluate whether the accumulation of cells in the sub-G1 peaks was due to the induction of apoptosis, we assessed the PARP cleavage, and as shown in Figure 6b lower panel, hMENA<sup>11a</sup> has a role in apoptosis as evidenced by the full length and cleaved pattern of PARP.

Tumors bearing high levels of the Bcl-2 family member BIM are more susceptible to PI3K inhibitor-mediated apoptosis and BIM has been proposed as a biomarker of apoptosis sensitivity.<sup>28</sup> In agreement with published results,<sup>29</sup> BEZ235 treatment did not increase BIM in either of the cell lines evaluated. Interestingly, at least in MDA-MB-361 cells, hMENA<sup>11a</sup> silencing determined an increase in BIM levels (Figure 6b), indicating that hMENA<sup>11a</sup> exerts an anti-apoptotic role and affects BIM expression.

hMENA<sup>11a</sup> sustains cancer cell resistance to PI3K inhibition in three-dimensional (3D) cultured BC cells

It is becoming increasingly evident that 3D cultures better reflect drug sensitivity *in vivo*.<sup>30,31</sup> Thus, we cultured MCF7-HER2 control

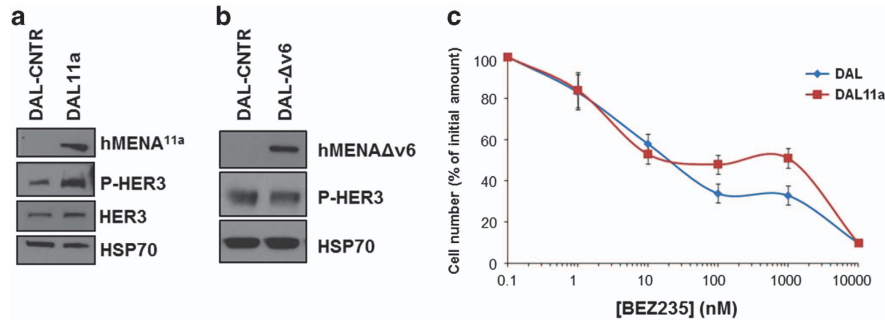


**Figure 5.** hMENA<sup>11a</sup> transfection in DAL cells increases HER3 activation and resistance to BEZ235 treatment. **(a)** WB analysis of DAL cells transfected with empty vector (CNTR) or hMENA<sup>11a</sup> (DAL11a) with the indicated antibodies. **(b)** WB analysis of lysates from DAL transfected with control vector (CNTR) or hMENA $\Delta$ v6 (DAL- $\Delta$ v6), with hMENA $\Delta$ v6 and P-HER3 antibodies. HSP70 was used as the loading control. **(c)** DAL and DAL11a cells were incubated with increasing concentrations of BEZ235 for a period of 72 h, fixed and stained with crystal violet. The effect on viability was reported as a percentage of the number of cells relative to control, defined as 100% survival. Each bar represents the mean  $\pm$  s.d. of three different experiments.

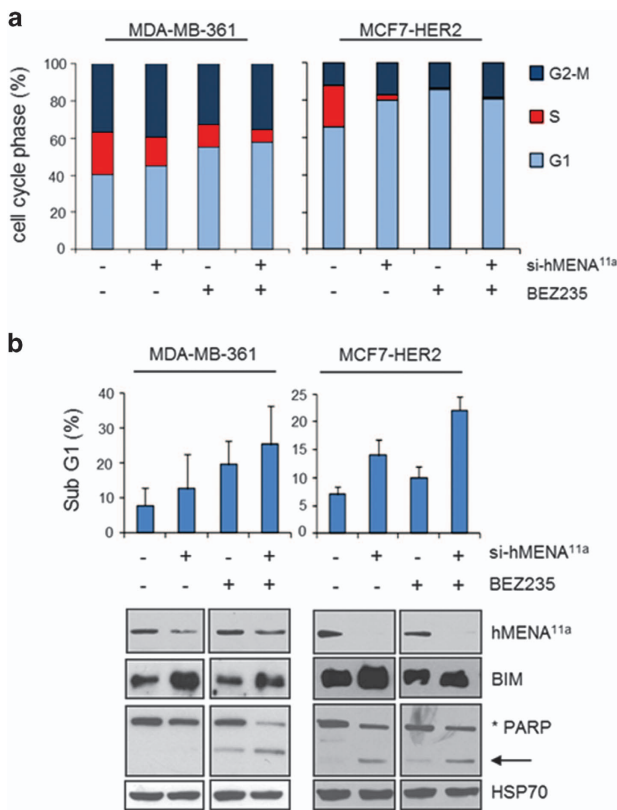


**Figure 6.** hMENA<sup>11a</sup> silencing reduces cell proliferation, induces cell apoptosis and sensitizes to PI3K inhibition. MDA-MB-361 and MCF7-HER2 were transfected with nontargeting si-RNA and hMENA<sup>11a</sup>-specific si-RNAs and treated with 0.5  $\mu$ M BEZ235 for 24 h. **(a)** Cells were subjected to cell cycle analysis by 5-bromo-2'-deoxyuridine incorporation assay, the percentage of cells in each phase of cell cycle is reported. **(b)** Upper panel: the percentage of cells in sub-G1 phase is reported. Each bar represents the mean  $\pm$  s.d. of three different experiments. **(b)** Lower panel: immunoblotting against hMENA<sup>11a</sup>, BIM and PARP antibodies is reported. HSP70 antibody was used as loading control. Asterisk: PARP uncleaved form; arrow: cleaved form.

and si-hMENA<sup>11a</sup> in a laminin-rich extracellular matrix and treated cells with BEZ235 for 48 h. Si-CNTR cells showed grape-like structures consistent with morphology previously described for HER2-overexpressing BC cells,<sup>32</sup> while si-hMENA<sup>11a</sup> cells formed

smaller colonies with a proportional increase in the number of 4'6-diamidino-2-phenylindole-stained cells (death cells) (Figure 7a). Morphological analysis at phase contrast microscopy and calcein staining (live cells) revealed that BEZ235 treatment leads to small colonies and dramatically reduces mass structures with the appearance of a major number of single cells in si-hMENA<sup>11a</sup> cells (Figure 7a). Immunohistochemical staining of 3D-cultured cells with Ki67 Ab confirmed that silencing of hMENA<sup>11a</sup> decreases Ki67 staining of cells (90  $\pm$  3,3 vs 65%  $\pm$  5), and BEZ235 treatment of hMENA<sup>11a</sup> silenced cells further reduces Ki67 staining (65  $\pm$  5 vs 38%  $\pm$  7,2) (Figure 7b).

This 3D analysis confirms the above-reported results with two-dimensional (2D) cultures and supports the data showing that hMENA<sup>11a</sup> silencing reduces cell proliferation and sensitizes cells to PI3K inhibition.

## DISCUSSION

The actin cytoskeleton architecture impacts many cellular processes and signaling pathways associated with cancer.<sup>11</sup> hMENA, an actin regulatory protein, undergoes splicing, and our group has described two alternatively expressed isoforms, hMENA<sup>11a</sup> and hMENA $\Delta$ v6, with opposite functions in cancer cell invasion.<sup>20</sup> hMENA<sup>11a</sup> is phosphorylated downstream of HER2 and EGFR after treatment with NRG-1 and EGF. hMENA<sup>11a</sup> cooperates with mitogenic signaling of the ErbB family receptors, and when hMENA and HER2 are both overexpressed, patients have a worse prognosis.<sup>15</sup> The role of hMENA<sup>11a</sup> in oncogenic signaling pathways has been poorly investigated and the kinase involved in hMENA<sup>11a</sup> phosphorylation has not yet been identified. Herein, we present data suggesting that the overexpression of the epithelial-associated hMENA<sup>11a</sup> isoform is correlated with HER3 overexpression and phosphorylation in HER2-positive tumors, is crucial for sustaining pro-survival pathways and participates in HER3 activation, influencing resistance mechanisms to PI3K/mTOR targeted therapies.

The success in obtaining specific hMENA<sup>11a</sup> isoform silencing allowed us to demonstrate that this isoform sustains different receptor tyrosine kinase signaling pathways. In particular, as evidenced by RPPA, in HER2-overexpressing BC cells, hMENA<sup>11a</sup> sustains the activation of ErbB family receptors, as evidenced by the downregulation of P-EGFR, P-HER2 and P-HER3 after specific silencing of this isoform. Even though the mechanisms involved still need to be elucidated, the results of RPPA suggest that hMENA<sup>11a</sup> is critical in sustaining the activation of relevant pathways involved in cell proliferation and apoptosis, as

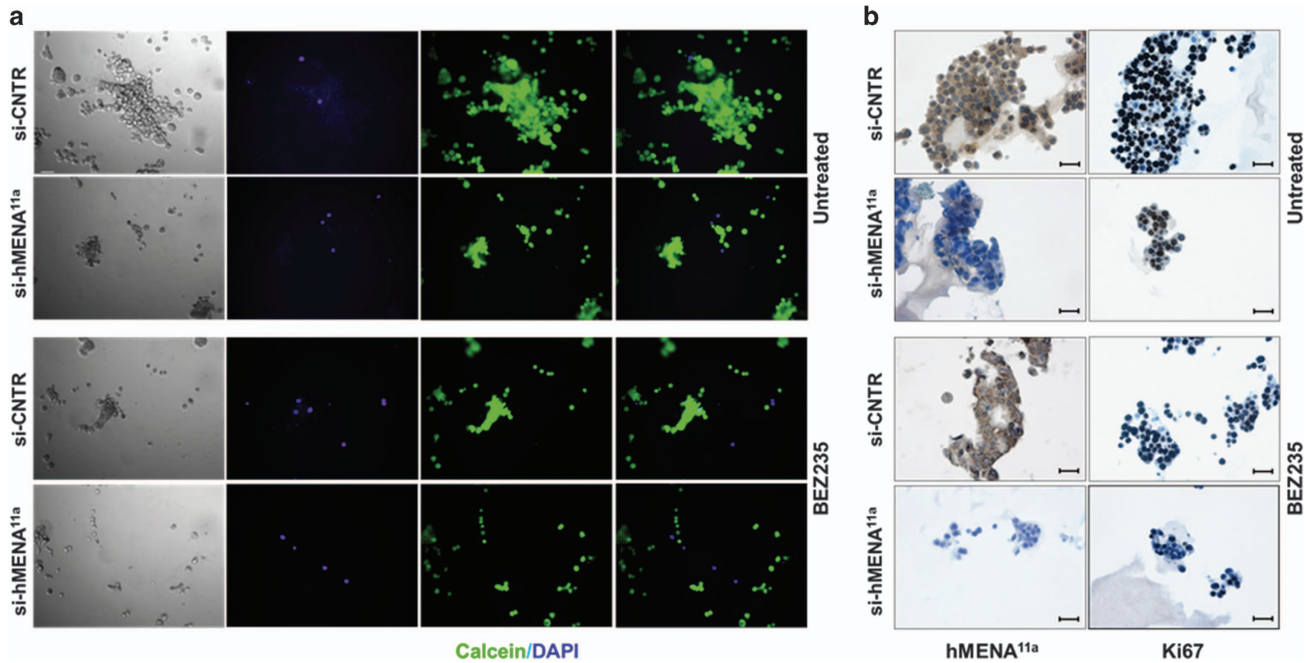


**Figure 7.** hMENA<sup>11a</sup> silencing reduces cell proliferation in 3D-cultured MCF7-HER2 cells and enhances antiproliferative effect of BEZ235. MCF7-HER2 cells were transfected with nontargeting si-RNA (si-CNTR) or hMENA<sup>11a</sup>-specific si-RNAs (si-hMENA<sup>11a</sup>), grown on laminin-rich extracellular matrix and untreated or treated with 0.5  $\mu\text{M}$  BEZ235 for 48 h. **(a)** Cells were stained with calcein (green) and 4'6-diamidino-2-phenylindole (blue) and imaged by Leica DM IRE2 microscopy. Magnification  $\times 20$ . Scale bar 50  $\mu\text{m}$ . **(b)** Matrigel/cells blocks were included in a Histogel 'sandwich' and embedded in paraffin, sectioned and immunostained with hMENA<sup>11a</sup> (left) and Ki67 (right) antibodies. Scale bar 30  $\mu\text{m}$ . Representative images of three different experiments are shown.

evidenced by the upregulation of critical molecules, such as H2AX and PARP, when hMENA<sup>11a</sup> is silenced.

On the basis of our previous data showing that NRG-1 phosphorylates hMENA<sup>11a</sup> (ref 15) and given the RPPA results, we performed phospho-proteomic analysis on cells silenced for hMENA<sup>11a</sup> and treated with NRG-1. hMENA<sup>11a</sup> silencing counteracts the NRG-1-mediated activation of different key molecules, including IRS1, reported to be recruited to HER3 following NRG-1 treatment.<sup>21</sup> Of note, the phosphorylation of IRS1 provides docking sites for the recruitment of key signaling pathways.<sup>21,33</sup> Interestingly, we found that NRG-1 was unable to activate HER3 signaling in cells lacking hMENA<sup>11a</sup>, suggesting a critical role of hMENA<sup>11a</sup> in HER3/AKT axis activation. This is relevant when considering the highlighted role of HER3 signaling in HER2-amplified BC cells.

Expression and signaling functions of HER3 are highly regulated through a multitude of mechanisms at the transcriptional, translational and posttranslational levels.<sup>34</sup>

Our data, showing that hMENA<sup>11a</sup> silencing decreases HER3 phosphorylation levels without influencing the RNA and protein levels, support the hypothesis that hMENA<sup>11a</sup> may participate in a posttranslational mechanism accounting for HER3 signaling activation without inducing the expression. At the moment, it is difficult to speculate on these findings. However, we can hypothesize that hMENA<sup>11a</sup> may participate in the highly dynamic nature of this HER family member, by affecting its localization and trafficking. Recently Vehlow *et al.*<sup>35</sup> reported that MENA cooperates with Lamellipodin and Endophilin to regulate F-actin-dependent EGFR endocytosis.

Of clinical relevance, our immunohistochemical results clearly support experimental data and for the first time, highlight the correlation among hMENA<sup>11a</sup>, HER3 activation and expression in HER2-overexpressing breast tumors. Although further studies are needed, we hypothesize that hMENA<sup>11a</sup> and its phosphorylation, affected by different growth factors, are relevant in the activation of the HER2/HER3 oncogenic unit.

Multiple studies have implicated the functions of HER3 as a major cause of treatment failure to targeted therapies and HER3 upregulation and activity have been proposed as a major compensatory feedback mechanism occurring after PI3K inhibition in HER2-overexpressing cell lines.<sup>5,6,36</sup>

Thus, we compared the effects of different PI3K inhibitors in HER2-overexpressing cell lines with respect to hMENA<sup>11a</sup> silenced cells. Notably, results at the RNA and protein levels highlight the role of hMENA<sup>11a</sup> in sustaining HER3 expression induced by PI3K inhibition. Indeed, silencing of hMENA<sup>11a</sup> was able to counteract the known compensatory effect of HER3 expression and activation exerted by the dual mTOR/PI3K inhibitor BEZ235. From a mechanistic point of view, downstream to PI3K inhibition, AKT when inhibited recruits the transcription factor FOXO3a to the HER3 promoter enabling HER3 expression.<sup>5,24</sup> Of note, we have found that FOXO3a nuclear accumulation determined by PI3K inhibition was impaired by hMENA<sup>11a</sup> silencing, with a crucial effect on HER3 transcription. The FOXO3a subcellular localization depends on the dynamic interactions with the Protein Phosphatase 2A (PP2A) and the scaffold proteins 14-3-3.<sup>37</sup> After inhibition of PI3K, the FOXO3a phosphorylation is no longer favored and PP2A and FOXO3a translocate into the nucleus after dissociation from 14-3-3.<sup>37</sup> Of relevance, as evaluated by ELM (Eukaryotic Linear Motifs) server (<http://elm.eu.org/>),<sup>38</sup> the hMENA<sup>11a</sup> sequence has four interacting motifs for 14-3-3, known to participate at the regulation of cytoskeleton.<sup>39</sup> Two out of the four motifs identified *in silico* are phospho-motifs present only in the 11a isoform, being located in the 21 aa sequence of the 11a peptide. Further studies, validating this predictive binding between hMENA<sup>11a</sup> and 14-3-3, will provide evidence supporting the hypothesis that hMENA<sup>11a</sup> via 14-3-3 binding may affect FOXO3a nuclear localization. Hence, the overexpression of this isoform and above all, its phosphorylation status may affect relevant molecular complexes involved in the transcription of HER3. hMENA<sup>11a</sup> amino-acid residues that are phosphorylated by growth factors<sup>15,16</sup> have not yet been identified. Also, the kinase

involved is yet to be identified. The 2D electrophoresis analysis clearly showed that PI3K inhibitor treatment, which does not affect hMENA<sup>11a</sup> expression, induces phosphorylation of hMENA<sup>11a</sup>, which in turn shifts its localization from the cytoplasm to the membrane. Consistent with these results, it has been recently reported that several of the phosphoproteins activated by PI3K pathway inhibitors are related to cytoskeletal reorganization and are proposed as candidate pharmacodynamic biomarkers for PI3K/AKT/mTOR drug development.<sup>40</sup> Although the mechanisms have to be further elucidated, our results suggest that hMENA<sup>11a</sup> overexpression and phosphorylation affect the HER3 phosphorylation and expression by mechanisms that are independent of each other. HER2 is the main kinase responsible for HER3 activation occurring after PI3K inhibition in HER2-overexpressing BC cells,<sup>4</sup> and we have previously reported that Trastuzumab treatment downregulates hMENA<sup>11a</sup> expression and phosphorylation,<sup>15</sup> thus, suggesting that hMENA<sup>11a</sup> overexpression and phosphorylation may sustain the HER2/HER3 dimer.

Recently, actin-binding proteins have been proposed as sensors and mediators of apoptosis, and remodeling of the actin cytoskeleton may enable tumor cells to escape normal apoptotic signaling.<sup>41</sup> No data are available on the role of hMENA or its isoforms in apoptotic processes, although we have previously reported that hMENA<sup>11a</sup> overexpression favors the proliferation rate of BC cells.<sup>16</sup> Our findings are consistent with the hypothesis that hMENA<sup>11a</sup> sustains an anti-apoptotic signaling in BC cells. Of clinical relevance, hMENA<sup>11a</sup> overexpression increases the resistance of BC cells to BEZ235 treatment, whereas its silencing sensitizes cells to BEZ235-induced death. Furthermore, the results that the hMENA<sup>11a</sup> silencing reduces the expression of the pro-apoptotic Bcl-2 family member BIM,<sup>42</sup> critical mediator of targeted therapy-induced apoptosis,<sup>28</sup> corroborate the hypothesis that hMENA<sup>11a</sup> promotes a survival advantage in BC cells.

The 3D models better recapitulate signaling pathways related to proliferation and survival<sup>43</sup> and have been reported as relevant systems to study cancer cell resistance to PI3K/mTOR inhibition.<sup>44</sup> Our monolayer culture results were validated in 3D, enforcing the role of hMENA<sup>11a</sup> in mechanisms of resistance to the dual inhibitor BEZ235.

Although further studies are required, our results hold promise for multi-fold clinical implications. We can speculate that hMENA<sup>11a</sup> expression may be proposed as a marker of HER3 activity, which lacks validated specific markers hampering the progress of HER3-targeted therapy.<sup>45</sup> Moreover, the specific expression of this hMENA isoform in combination with BIM may permit the selection of patients less likely to respond or those who may derive maximal benefit from therapies including PI3K/mTOR inhibitors. There is hope that the identification of drugs able to shut down hMENA<sup>11a</sup> activity may lead to the design of more effective antiproliferative therapies in BC.

## MATERIALS AND METHODS

### Cell lines and treatments

The human breast carcinoma cell lines MDA-MB-361 and MCF7 were obtained from the ATCC; MCF7-HER2 stable transfectants were obtained as previously described.<sup>15</sup> DAL cell line, DAL11a and DALΔv6 transfectants were obtained as previously reported.<sup>20,46</sup> All cell lines were routinely tested for ER status, morphologically checked by microscope, growth curve analysis by 3H-Thymidine incorporation assay and Mycoplasma detection (Roche, Monza, Italy).

NRG-1 (PeproTech, Rocky Hill, NJ, USA) was added to serum-starved cells at a concentration of 10 ng/ml. BEZ235 (0.5 μM, Selleck Chemicals, Houston, TX, USA), XL147 (20 μM, Selleck Chemicals) and LY294002 (10 μM, Cell Signaling Technology, Danvers, MA, USA) were used.

### Small-interfering RNA (siRNA) treatment

Cells were transfected using Lipofectamine 2000 (Invitrogen, Carlsbad, CA, USA) with 100 nmol/l of ON-TARGETplus Nontargeting Control Pool (GE-Healthcare, Dharmacon, Lafayette, CO, USA), or HER3 siRNA. Specific hMENA<sup>11a</sup> silencing was performed by transfecting cells with a mix of three siRNAs (30 pmol each) each matching 21 nucleotides within the 11a exon sequence. The siRNAs sequences used are reported in Supplementary Table 6.

For NRG-1 stimulation, 24 h after the transfection, cells were serum-starved for 18 h and then treated with NRG-1; for PI3K inhibitor treatments, 48 h after the transfection, cells were treated with XL147 in 2.5% serum containing medium or with BEZ235 or LY294002 in complete medium. Cells were processed 72 h after the transfection.

### Reverse phase protein array

Protein lysate preparation and RPPA were performed on biological triplicate samples, as previously reported.<sup>47</sup> Supplementary Table 1 reports detailed information concerning the antibodies used.

Spot intensity was analyzed by MicroVigene software V5.1 (VigeneTech, North Billerica, MA, USA), and normalized to total protein and standardized. RPPA data were subjected to unsupervised statistical analysis (average method) using JMP V10.0.2 (SAS Institute, Cary, NC, USA). Statistically significant endpoints were evaluated using the multiple comparison Dunnett's test. *P* values < 0.05 were considered significant. The lists of total significant and nonsignificant endpoints were reported in Supplementary Tables 2 and 3.

### WB analysis

WB was performed as reported.<sup>15</sup> Nuclear and cytoplasmic fractions were prepared using NE-PER Nuclear Cytoplasmic Extraction Reagent kit (Pierce, Rockford, IL, USA). Anti-hMENA<sup>11a</sup>, pan-hMENA and hMENAΔv6 were used as already described.<sup>14,15,20</sup> Anti-HER3 #12708, P-HER3 (Y1289) #4791, P-AKT (S473) #4060, AKT #4685, P-S6 (S240/244) #2215, S6 #2217, BIM #2819, PARP #9542 (Cell Signaling Technology), anti H3 #Ab-1791 (Abcam, Cambridge, UK), anti-β actin #A4700 (Sigma-Aldrich, Poole, UK), HSP70 #sc-24 (Santa Cruz Biotechnology, Inc, Santa Cruz, CA, USA), anti-FOXO3a #04-1007 (EMD Millipore Corporation, St Charles, MO, USA) were used.

### Immunohistochemistry

HER2, ER, PgR and Ki67 status and hMENA<sup>11a</sup> expression were assessed on tissues from 49 HER2-positive BC patients as previously reported.<sup>20</sup> HER3 (#NCL-cerbB-3, Novocastra Leica, Menarini, Florence, Italy) and P-HER3 (Cell Signaling Technology) antibodies were used. For HER3, P-HER3 and hMENA<sup>11a</sup>, an immunohistochemistry (IHC) score of 2/3 on the membrane or cytoplasm was defined as positive. For statistical analysis, negative (score 0/1) and positive (score 2/3) groups were created. Evaluation of the IHC results was performed independently by two investigators (MM, ADB) blinded to patient data.

### RNA extraction and real-time PCR

Total RNA extraction and cDNA synthesis were performed as reported.<sup>20</sup> HER3 primers used were: 5'-GGGGAGTCTTGCCAGGAG-3' and 5'-CATTGGGTGTAGAGACTGGAC-3'. GAPDH primers were used as an internal control. qRT-PCR was performed with 10 ng cDNA in ABI Prism 7900 Real-time PCR system using SYBR Green PCR Master Mix (Applied Biosystems, Princeton, NJ, USA). Gene expression was calculated using the equation  $2^{-\Delta\Delta Ct}$ .<sup>48</sup>

### Immunofluorescence

Cells transfected with siRNAs and/or treated with PI3K inhibitors were fixed and permeabilized as previously described.<sup>20</sup> Cells were stained with anti-hMENA<sup>11a</sup> and/or anti-FOXO3a antibodies. Nuclei were stained with 4',6-diamidino-2-phenylindole (Invitrogen). Immunofluorescence was analyzed by Leica DM IRE2 microscopy with Leica FW 4000 software (Leica, Solms, Germany).

### 2D electrophoresis

2D electrophoresis was performed as previously described.<sup>15</sup>



### Crystal violet assay

Cells ( $5 \times 10^4$ ) seeded in triplicates in 24-well plates were treated with increasing doses of BEZ235 for 72 h. Cells were fixed with 4% formaldehyde and stained with 0.1% crystal violet (Sigma). The dye was subsequently extracted with 10% acetic acid, its absorbance was determined (570 nm) and the percentages of surviving cells relative to control, defined as 100% survival, were reported. IC50 values were calculated by Calcsyn software.

### <sup>3</sup>H-Thymidine incorporation assay

<sup>3</sup>H-Thymidine incorporation assay was performed as reported.<sup>15</sup>

### Cell cycle analysis

Cell cycle was analyzed with FITC BrdU-Flow KIT (BD Pharmingen, San Jose, CA, USA) according to the manufacturer's instructions. Cells were acquired on FACSCanto II Flow Cytometer (BD Biosciences, San Jose, CA, USA).

### Live/dead assay and IHC in 3D cell cultures

Cells ( $1 \times 10^5$ ) were seeded on top of a growth factor reduced reconstituted basement membrane Matrigel (BD Pharmingen) containing 5% (vol/vol) laminin-rich extracellular matrix and plated in six-well plates for live/dead assay or into an eight-well plastic-chambered glass microscope slide (Thermo Scientific Nunc Lab-Tek II Chamber Slide System, Thermo Fisher Scientific, Waltham, MA, USA) for IHC. The day after, 0.5  $\mu$ M BEZ235 was added for 48 h. For live/dead assay, cells were incubated for 30 min at 37 °C with 100  $\mu$ M calcein AM (Invitrogen) and 0.1  $\mu$ g/ml 4'-diamidino-2-phenylindole to stain viable and nonviable cells, respectively. Intensity of fluorescence was assessed as reported above. For IHC, 3D cell cultures were processed as previously reported<sup>49</sup> and immunostained with hMENA<sup>11a</sup> and Ki67 (#M724001, DAKO, Milan, Italy) antibodies.

### Statistical analysis

All experiments were repeated a minimum of three times. Data are expressed as the mean  $\pm$  s.d. Statistical significance was determined by Student's *t* test (two-tailed) comparison between two groups of datasets, with similar variance. Asterisks indicate significant differences of experimental groups compared with the corresponding control condition ( $P < 0.05$ ). To assess the relationship between categorical variables, Fisher's exact test was used when appropriate. A *P* value of  $< 0.05$  was considered statistically significant. To calculate the sample size for immunohistochemical study, we based on the percentage of HER2/HER3 positivity with respect to hMENA<sup>11a</sup> expression in BC cell lines.<sup>20,50</sup> The proportion of HER2/HER3 positivity was equal to 80% in hMENA<sup>11a</sup>-positive BC and 40% in hMENA<sup>11a</sup>-negative BC. Applying a two-sided Z-test with pooled variance, assuming a statistical power equal to 80% and a significance level equal to 0.05, we needed to recruit a minimum of 46 patients.

Statistical analyses were carried out using SPSS software (SPSS version 21, SPSS Inc., Chicago, IL, USA). The data presented in some figures are from a representative experiment, which was qualitatively similar in the replicate experiments.

### CONFLICT OF INTEREST

The authors declare no conflict of interest.

### ACKNOWLEDGEMENTS

We thank Dr C Rinaldo for her helpful suggestions, Dr M Panetta for her support, Dr I Terrenato for statistical analysis of data, Mrs G Falasca for technical support and Mrs MV Sarcone for secretarial assistance. This work was supported by the Associazione Italiana per la Ricerca sul Cancro (AIRC) 5x1000 Grants 12182 and 9979 and IG 11631 (to PN).

### REFERENCES

- 1 Arteaga CL, Engelman JA. ERBB receptors: from oncogene discovery to basic science to mechanism-based cancer therapeutics. *Cancer Cell* 2014; **25**: 282–303.
- 2 Rexer BN, Arteaga CL. Optimal targeting of HER2-PI3K signaling in breast cancer: mechanistic insights and clinical implications. *Cancer Res* 2013; **73**: 3817–3820.
- 3 Fruman DA, Rommel C. PI3K and cancer: lessons, challenges and opportunities. *Nat Rev Drug Discov* 2014; **13**: 140–156.

- 4 Serra V, Scaltriti M, Prudkin L, Eichhorn PJ, Ibrahim YH, Chandarlapaty S *et al*. PI3K inhibition results in enhanced HER signaling and acquired ERK dependency in HER2-overexpressing breast cancer. *Oncogene* 2011; **30**: 2547–2557.
- 5 Chandarlapaty S, Sawai A, Scaltriti M, Rodrik-Outmezguine V, Grbovic-Huezo O, Serra V *et al*. AKT inhibition relieves feedback suppression of receptor tyrosine kinase expression and activity. *Cancer Cell* 2011; **19**: 58–71.
- 6 Chakrabarty A, Sánchez V, Kuba MG, Rinehart C, Arteaga CL. Feedback upregulation of HER3 (ErbB3) expression and activity attenuates antitumor effect of PI3K inhibitors. *Proc Natl Acad Sci USA* 2012; **109**: 2718–2723.
- 7 Amin DN, Campbell MR, Moasser MM. The role of HER3, the unpretentious member of the HER family, in cancer biology and cancer therapeutics. *Sem Cell Dev Biol* 2010; **21**: 944–950.
- 8 Hellyer NJ, Cheng K, Koland JG. ErbB3 (HER3) interaction with the p85 regulatory subunit of phosphoinositide 3-kinase. *Biochem J* 1998; **333**: 757–763.
- 9 Hellyer NJ, Kim MS, Koland JG. Heregulin-dependent activation of phosphoinositide 3-kinase and Akt via the ErbB2/ErbB3 co-receptor. *J Biol Chem* 2001; **276**: 42153–42161.
- 10 Amin DN, Sergina N, Ahuja D, McMahon M, Blair JA, Wang D *et al*. Resiliency and vulnerability in the HER2-HER3 tumorigenic driver. *Sci Transl Med* 2010; **2**: 16ra7.
- 11 Olson EN, Nordheim A. Linking actin dynamics and gene transcription to drive cellular motile functions. *Nat Rev Mol Cell Biol* 2010; **11**: 353–365.
- 12 Gertler FB, Niebuhr K, Reinhard M, Wehland J, Soriano P. Mena a relative of VASP and Drosophila Enabled, is implicated in the control of microfilament dynamics. *Cell* 1996; **87**: 227–239.
- 13 Bear JE, Loureiro JJ, Libova I, Fässler R, Wehland J, Gertler FB. Negative regulation of fibroblast motility by Ena/VASP proteins. *Cell* 2000; **101**: 717–728.
- 14 Di Modugno F, Mottolese M, Di Benedetto A, Conidi A, Novelli F, Perracchio L *et al*. The cytoskeleton regulatory protein hMena (ENAH) is overexpressed in human benign breast lesions with high risk of transformation and human epidermal growth factor receptor-2-positive/hormonal receptor-negative tumors. *Clin Cancer Res* 2006; **12**: 1470–1478.
- 15 Di Modugno F, Mottolese M, DeMonte L, Trono P, Balsamo M, Conidi A *et al*. The cooperation between hMena overexpression and HER2 signalling in breast cancer. *PLoS One* 2010; **5**: e15852.
- 16 Di Modugno F, DeMonte L, Balsamo M, Bronzi G, Nicotra MR, Alessio M *et al*. Molecular cloning of hMena (ENAH) and its splice variant hMena 11a: epidermal growth factor increases their expression and stimulates hMena 11a phosphorylation in breast cancer cell lines. *Cancer Res* 2007; **67**: 2657–2665.
- 17 Urbanelli L, Massini C, Orlacchio C, Orlacchio A, Bernardi G, Orlacchio A. Characterization of human Enah gene. *Biochim Biophys Acta* 2006; **1759**: 99–107.
- 18 Tani K, Sato S, Sukezane T, Kojima H, Hirose H, Hanafusa H *et al*. Abl interactor 1 promotes tyrosine 296 phosphorylation of mammalian enabled (Mena) by c-Abl kinase. *J Biol Chem* 2003; **278**: 21685–21692.
- 19 Goswami S, Philippar U, Sun D, Patsialou A, Avraham J, Wang W *et al*. Identification of invasion specific splice variants of the cytoskeletal protein Mena present in mammary tumor cells during invasion in vivo. *Clin Exp Metastasis* 2009; **26**: 153–159.
- 20 Di Modugno F, Iapicca P, Boudreau A, Mottolese M, Terrenato I, Perracchio L *et al*. Splicing program of human MENA produces a previously undescribed isoform associated with invasive, mesenchymal-like breast tumors. *Proc Natl Acad Sci USA* 2012; **109**: 19280–19285.
- 21 Knowlden JM, Gee JM, Barrow D, Robertson JF, Ellis IO, Nicholson RI *et al*. erbB3 recruitment of insulin receptor substrate 1 modulates insulin-like growth factor receptor signalling in oestrogen receptor-positive breast cancer cell lines. *Breast Cancer Res* 2011; **13**: R93.
- 22 Maira SM, Stauffer F, Brueggen J, Furet P, Schnell C, Fritsch C *et al*. Identification and characterization of NVP-BEZ235, a new orally available dual phosphatidylinositol 3-kinase/mammalian target of rapamycin inhibitor with potent in vivo antitumor activity. *Mol Cancer Ther* 2008; **7**: 1851–1863.
- 23 Vlahos CJ, Matter WF, Hui KY, Brown RF. A specific inhibitor of phosphatidylinositol 3-kinase, 2-(4-morpholinyl)-8-phenyl-4H-1-benzopyran-4-one (LY294002). *J Biol Chem* 1994; **269**: 5241–5248.
- 24 Garrett JT, Olivares MG, Rinehart C, Granja-Ingram ND, Sánchez V, Chakrabarty A *et al*. Transcriptional and posttranslational up-regulation of HER3 (ErbB3) compensates for inhibition of the HER2 tyrosine kinase. *Proc Natl Acad Sci USA* 2011; **108**: 5021–5026.
- 25 Shapiro GI, Rodon J, Bedell C, Kwak EL, Baselga J, Braña I *et al*. Phase I safety, pharmacokinetic, and pharmacodynamic study of SAR245408 (XL147), an oral pan-class I PI3K inhibitor, in patients with advanced solid tumors. *Clin Cancer Res* 2014; **20**: 233–245.
- 26 Di Modugno F, Bronzi G, Scanlan MJ, Del Bello D, Cascioli S, Venturo I *et al*. Human Mena protein, a serex-defined antigen overexpressed in breast cancer eliciting both humoral and CD8 T-cell immune response. *Int J Cancer* 2004; **109**: 909–918.
- 27 Serra V, Markman B, Scaltriti M, Eichhorn PJ, Valero V, Guzman M *et al*. NVP-BEZ235, a dual PI3K/mTOR inhibitor, prevents PI3K signaling and inhibits the

- growth of cancer cells with activating PI3K mutations. *Cancer Res* 2008; **68**: 8022–8030.
- 28 Faber AC, Corcoran RB, Ebi H, Sequist LV, Waltman BA, Chung E *et al*. BIM expression in treatment-naïve cancers predicts responsiveness to kinase inhibitors. *Cancer Discov* 2011; **1**: 352–365.
- 29 Bean GR, Ganesan YT, Dong Y, Takeda S, Liu H, Chan PM *et al*. PUMA and BIM are required for oncogene inactivation-induced apoptosis. *Sci Signal* 2013; **6**: ra20.
- 30 Howes AL, Chiang GG, Lang ES, Ho CB, Powis G, Vuori K *et al*. The phosphatidylinositol 3-kinase inhibitor, PX-866, is a potent inhibitor of cancer cell motility and growth in three-dimensional cultures. *Mol Cancer Ther* 2007; **6**: 2505–2514.
- 31 Polo ML, Arnoni MV, Riggio M, Wargon V, Lanari C, Novaro V. Responsiveness to PI3K and MEK inhibitors in breast cancer. Use of a 3D culture system to study pathways related to hormone independence in mice. *PLoS One* 2010; **5**: e10786.
- 32 Kenny PA, Lee GY, Myers CA, Neve RM, Semeiks JR, Spellman PT *et al*. The morphologies of breast cancer cell lines in three-dimensional assays correlate with their profiles of gene expression. *Mol Oncol* 2007; **1**: 84–96.
- 33 Sun XJ, Rothenberg P, Kahn CR, Backer JM, Araki E, Wilden PA *et al*. Structure of the insulin receptor substrate IRS-1 defines a unique signal transduction protein. *Nature* 1991; **352**: 73–77.
- 34 Amin DN, Sergina N, Lim L, Goga A, Moasser MM. HER3 signalling is regulated through a multitude of redundant mechanisms in HER2-driven tumour cells. *Biochem J* 2012; **447**: 417–425.
- 35 Vehlou A, Soong D, Vizcay-Barrena G, Bodo C, Law AL, Perera U *et al*. Endophilin, Lamellipodin, and Mena cooperate to regulate F-actin-dependent EGF-receptor endocytosis. *EMBO J* 2013; **32**: 2722–2734.
- 36 Sergina NV, Rausch M, Wang D, Blair J, Hann B, Shokat KM *et al*. Escape from HER-family tyrosine kinase inhibitor therapy by the kinase-inactive HER3. *Nature* 2007; **445**: 437–441.
- 37 Singh A, Ye M, Bucur O, Zhu S, Tanya Santos M, Rabinovitz I *et al*. Protein phosphatase 2A reactivates FOXO3a through a dynamic interplay with 14-3-3 and AKT. *Mol Biol Cell* 2010; **21**: 1140–1152.
- 38 Dinkel H, Michael S, Weatheritt RJ, Davey NE, Van Roey K, Altenberg B *et al*. ELM—the database of eukaryotic linear motifs. *Nucleic Acids Res* 2012; **40**: D242–D251.
- 39 Boudreau A, Tanner K, Wang D, Geyer FC, Reis-Filho JS, Bissell MJ. 14-3-3 $\sigma$  stabilizes a complex of soluble actin and intermediate filament to enable breast tumor invasion. *Proc Natl Acad Sci USA* 2013; **110**: E3937–E3944.
- 40 Andersen JN, Sathyanarayanan S, Di Bacco A, Chi A, Zhang T, Chen AH *et al*. Pathway-based identification of biomarkers for targeted therapeutics: personalized oncology with PI3K pathway inhibitors. *Sci Transl Med* 2010; **2**: 43ra55.
- 41 Desouza M, Gunning PW, Stehn JR. The actin cytoskeleton as a sensor and mediator of apoptosis. *Bioarchitecture* 2012; **2**: 75–87.
- 42 O'Connor L. Bim: a novel member of the Bcl-2 family that promotes apoptosis. *EMBO J* 1998; **17**: 384–395.
- 43 Weigelt B, Ghajar CM, Bissell MJ. The need for complex 3D culture models to unravel novel pathways and identify accurate biomarkers in breast cancer. *Adv Drug Deliver Rev* 2014; **69-70**: 42–51.
- 44 Muranen T, Selfors LM, Worster DT, Iwanicki MP, Song L, Morales FC *et al*. Inhibition of PI3K/mTOR leads to adaptive resistance in matrix-attached cancer cells. *Cancer Cell* 2012; **21**: 227–239.
- 45 Gala K, Chandarlapaty S. Molecular pathways: HER3 targeted therapy. *Clin Cancer Res* 2014; **20**: 1410–1416.
- 46 Nisticò P, De Berardinis P, Morrone S, Alonzi T, Buono C, Ventura I *et al*. Generation and characterization of two human alpha/beta T cell clones. Recognizing autologous breast tumor cells through an HLA- and TCR/CD3-independent pathway. *J Clin Invest* 1994; **94**: 1426–1431.
- 47 Federici G, Gao X, Slawek J, Arodz T, Shitaye A, Wulfskuhle JD *et al*. Systems analysis of the NCI-60 cancer cell lines by alignment of protein pathway activation modules with “-OMIC” data fields and therapeutic response signatures. *Mol Cancer Res* 2013; **11**: 676–685.
- 48 Livak KJ, Schmittgen TD. Analysis of relative gene expression data using real-time quantitative PCR and the 2(-Delta Delta C(T)) Method. *Methods* 2001; **25**: 402–408.
- 49 Pinto MP, Jacobsen BM, Horwitz KB. An immunohistochemical method to study breast cancer cell subpopulations and their growth regulation by hormones in three-dimensional cultures. *Front Endocrinol (Lausanne)* 2011; **2**: 15.
- 50 Morrison MM, Hutchinson K, Williams MM, Stanford JC, Balko JM, Young C *et al*. ErbB3 downregulation enhances luminal breast tumor response to antiestrogens. *J Clin Invest* 2013; **123**: 4329–4343.

Supplementary Information accompanies this paper on the Oncogene website (<http://www.nature.com/onc>)